International Journal of Wireless Information Networks (2018) 25:146–156
https://doi.org/10.1007/s10776-018-0389-0

# WiDriver: Driver Activity Recognition System Based on WiFi CSI

**Shihong Duan**[1] · **Tianqing Yu**[1] · **Jie He**[1]

Received: 24 May 2017 / Accepted: 8 January 2018 / Published online: 5 February 2018


**Abstract**
Driver is the most active factor in people–vehicle–road system, so the driver activity monitoring has become increasingly important to support the driver assistant system application. The possibility of using device-free sensing technology for driver activity recognition in a simulated driving environment is investigated in this paper. We present WiDriver, among the first efforts to employ channel state information (CSI) amplitude variation data to intelligently estimate driving actions with commodity WiFi devices. The WiDriver proposes the scheme of screening sensitive input data from original CSI matrix of WiFi signals based on BP neural network algorithm; and the continuous driving activities classification algorithm by introducing the posture sequence, driving context finite automate model. Our experimental driving study in carriage with 5 subjects shows that the sensitive input selection scheme can achieve high accuracy of 96.8% in posture recognition and the continuous action classification algorithm can reach 90.76% maneuver operation detection rate.

**Keywords** CSI · RSSI · Activity recognition · Neural network

## 1 Introduction

Driver is the most active factor in people–vehicle–road system [1]. So the driver activity recognition is crucial for driving assistant system to determine the operation and safety prompt in conditional autonomous driving scenarios. Specially, the promise of device-free activity recognition system based on wireless signals is the lure that attracts researchers to this promising technology.

Previous work always use video [2, 3] and wearable equipment [4, 5] to classify the driver activity. Computer vision based driver operation monitoring systems use cameras installed in some specific places to either capture images or video sequences for activities recognition. Recent advances in infra-red LED and depth camera like Microsoft Kinect [5], have enlarged video-based application scope, for example working even in a dark environment. However, there are still a set of open issues to be resolved, such as privacy concern, requirement for line of sight and intensive computation for real-time processing. Wearable sensor based driver action recognition systems were among the efforts about classifying driver operation. These detection systems can only work on the premise that all the devices are worn or carried by the subject during driving. The always-on-the-body requirements make the driver difficult to comply with.

Auto manufacturers are increasingly integrating Wi-Fi into new vehicles. Roughly one-quarter of all new cars offer built-in wireless Internet connections, according to Edmunds.com. Wi-Fi communications in vehicles, whether from the factory or in aftermarket devices, will increase from 6.9 million per year in 2015 to 61 million per year in 2020, and this will usher in a new era of consumer services and applications. Also, the existence and movement of humans will affect the channel state [7]. So it is inspiring to identify driver motions by leveraging the WiFi signals transmitted between the commercial WiFi devices.

In fact, using WiFi signals to detect the human activities has attracted the attention of many researchers. While [8, 9] explore and use WiFi RF signal to recognize different body or hand gestures, they use dedicated instruments to collect special RF signals, which are not accessible with commodity WiFi devices. With the CSI tractable on commodity WiFi devices [10, 11], some recent work uses CSI values to recognize various macro aspects of human movements such as falling down [12], daily household activities [13], detection of human presence [14], and counting

✉ Jie He
hejie@ustb.edu.cn

[1] School of Computer and Communication Engineering, University of Science and Technology Beijing, Beijing, China

people number in a crowd [15]. These schemes recognize the macro-movements such as falling down or full-body/limb gestures. The detection algorithm are diverse according to different sensitive eigenvalues, not can be directly adapted to recognize driver operation on steering wheel. Some schemes can capture the micro-movements. Wang et al. propose WiHear [16] that uses CSI values recognizes the shape of mouth to detect whether a person is uttering one of a set of nine predefined syllables; but it uses special purpose directional antennas with stepper motors. Kamran Ali describes WiKey [17] that achieves high accuracy rate for detecting the keystroke and classifying single keys. Wang et al. [18] and Liu et al. [19] exploits CSI to detect the breathing rate. Each scheme designed special feature extraction algorithm to get most sensitive data for specific application, such as keystroke or human respiration detection. Xu et al. [20] summarizes selection of sensitive feature data in human activity recognition in some special scene. The said schemes of eigenvalue selection cannot be used in our scheme to pick up sensitive input for driver activity recognition.

In this paper, we show for the first time that signals transmitted between WiFi commodity devices can also be exploited to recognize driver activities. Firstly, we intensively study the relationship between the driver activities and the channel features, such as amplitude, phase, and RSSI information in CSI matrix. We find that the amplitude with RSS is a more sensitive input than amplitude only or phase only for human activity recognition in car in acceptable processing time. Furthermore, we discover a Driving Context Finite Automata (DCFA) model of continuous operation action, and introduce the DCFA model into action recognition algorithm. By leveraging the findings about the driver activities, we realize the WiDriver system feasible to detect driver actions based on the Wi-Fi RF signal streams.

Our main contribution is to present WiDriver, a driver action recognition system using Commercial Off-The-Shelf (COTS) Wi-Fi devices. In the evaluation process, we build a driver action database of 5 human subjects with 11 static gestures and 7 continuous actions. WiDriver achieves more than 96.8% accuracy rate for detecting the static gesture and 90.76% recognition accuracy for classifying continuous operation action. The WiDriver is the first demo system to use CSI data in driver maneuver recognition.

The remainder of this paper is organized as follows. Section 2 presents the system architecture, Sect. 3 describes selection of sensitive input from CSI matrix, Sect. 4 details action recognition algorithm based on DCFA model, Sect. 5 discusses the experimental setup and results. Section 6 concludes this paper and provides suggestions for future research.

## 2 System Overview

Most of the traffic accidents are, at least in part, due to driver error. Monitoring driver's behavior plays a critical role, especially supports the driver assistant system application extension. Normal driving assistant system uses {*GPS location, real-time traffic, city map*} as input set to calculate the optimal path according to current traffic and destination. But whether the driver is following the path or not will be detected later until GPS location is updated. So, driver activities of operating the wheel is another important potential input, then driving assistant system can decide if the driver will follow the route or drive safely.

### 2.1 Driver Activity Overview

Ohn-Bar [21] presented that 37% of the drivers admit to having sent or received text messages, with 18% doing so regularly while operating a vehicle. Furthermore, 86% of drivers report eating or drinking, and common GPS system interaction, surfing the internet are also reported. This section defines 11 kinds of driver arm and hand postures related to operating the wheel, shown in Fig. 1. We conceptualize driver posture in terms of an operation tuples defines as posture = <motion-target> . The *posture operation* tuple represents the goal-oriented motion of the driver arms and hands. Different motion turns the steering wheel to different angle. Driving straight means that steering wheel rotation

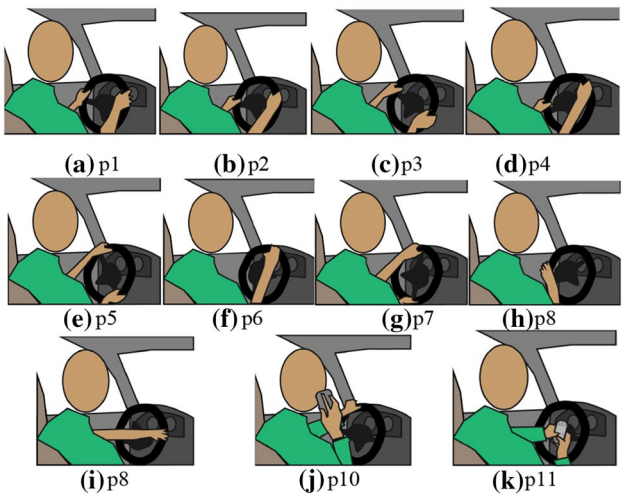


**Fig. 1** Posture operation tuple value: **a** p1 = <stay-wheel: 0°>, **b** p2 = <turning left-wheel: − 20°>, **c** p3 = <turning right-wheel: + 20°>, **d** p4 = <turning left-wheel: − 40°>, **e** p5 = <turning right-wheel: + 40°>, **f** p6 = <turning left-wheel: − 80°>, **g** p7 = <turning right-wheel: + 80°>, **h** p8 = <turning left-wheel: − 270°>, **i** p9 = <turning right-wheel: + 270°>, **j** P10 = <raise &call- wheel: 0°>, **k** P11 = <send_message-wheel: 0°>

angle is 0, turning left corresponds to negative angle, and turning right corresponds to positive angle.

The *action* set contains basic hand-arm action atoms for driver wheel maneuver operation, such as turn right, turn left, stay, phone call and send message. This paper defined normal 8 kinds of continuous action of operating steering wheel for tracking driver maneuvers. The different steering maneuvers are described with set action = {a0, a1, a2, a3, a4, a5, a6 a7} as shown in Fig. 2, and $t_{i0}$ denotes the start time of $a_i$, $t_{i1}$ is the end time of $a_i$.

## 2.2 System Architecture

To identify driver posture and vehicle steering maneuvers, we focus on statistical analysis of the Wi-Fi signal variance in vehicle compartment. The key intuition is that while operating the steering wheel, the hands and arms of a driver move in a unique formation and direction, thus generate a unique pattern in the time-series of Channel State Information (CSI) values. CSI can be obtained from commodity Wi-Fi network interface cards (NICs), e.g., Intel 5300, Atheors 9580, etc. Each action of the driver introduces relative unique multi-path distortions in Wi-Fi signals and this uniqueness of CSI waveform can be exploited to recognize action. Due to the high data rates supported by modern Wi-Fi devices, Wi-Fi cards provide enough CSI values within the duration of a driver operation to construct a high-resolution CSI waveform for recognition of driver activities.

The paper proposed a WiFi CSI signal based driver action recognition system called WiDriver. WiDriver consists of two Commercial Off-The-Shelf (COTS) WiFi devices, a sender (such as a router) and a receiver (such as a laptop), as shown in Fig. 3. The sender is put on left side of dash panel, and the receiver is deployed on right side of dash panel in front of co-pilot position. The sender emits signals and the receiver deployed in continuously receives CSI signals. CSI values quantify the aggregate effect of wireless phenomena such as fading, multi-paths, and Doppler shift on the wireless signals in a given environment. The driver's operation can change the channel environment, resulting in unique channel variance in the CSI values. The WiDriver leverage the sensitive data from CSI original matrix to classify the driver's arms-and-hands postures and steering operation maneuvers.

## 2.3 Theory Behind the WiDriver

It is known that the movement of the humans and objects change the multipath characteristic of the wireless channel and hence the estimated channel will have a different amplitude and phase. But activities of hands and arms to control the wheel can really be distinguished from the CSI data? Zhang [22] introduced theoretical Fresnel Zone Model which can capture subtle body displacement on the receiving RF signal at the granularity of sub wavelengths and enable centimeter-scale human activity recognition.

Received signal paths can be divided into static and dynamic paths, the received signal H(f,t) can be denoted as the following equation

$$\mathrm{H(f,t)} = H_s(f,t) + H_d(f,t) \tag{1}$$

where the static vector $H_s(f,t)$ is the sum of signals from static paths, and the dynamic vector $H_d(f, t)$ is introduced by the reflection signal from the moving object. The effect of static objects in car carriage on wireless channel will described in $H_s(f, t)$, valid CSI fluctuation expressed by $H_d(f, t)$ is used for action recognition.

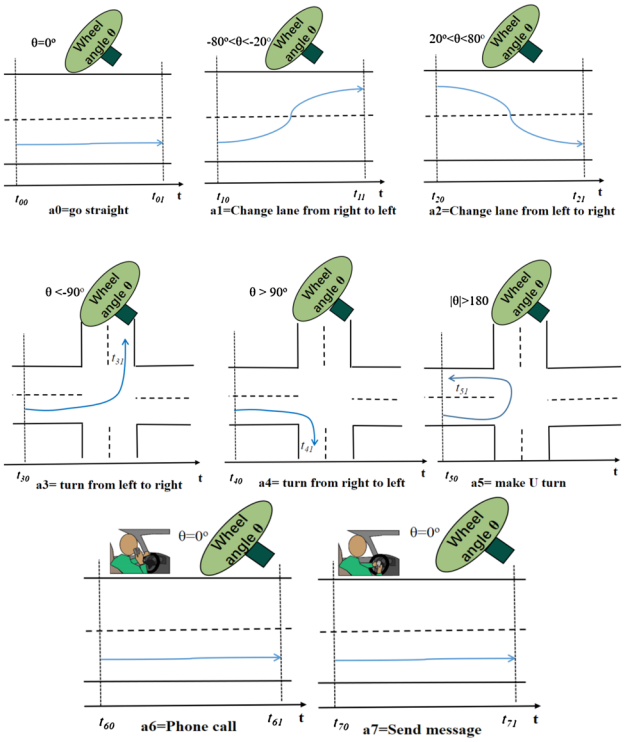


**Fig. 2** Definition of driver continuous action

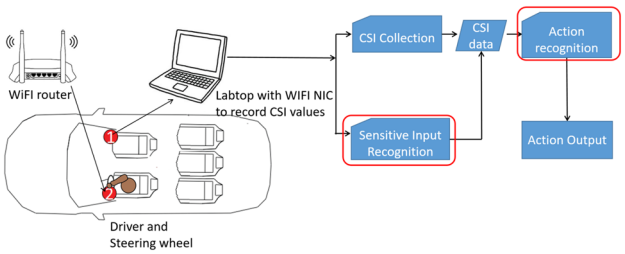


**Fig. 3** WiDriver schematic

For subtle centimeter-scale human motion, that is the activity amplitude is less than wavelength, the frequency diversity can be exploited to enhance sensing. Starting from a certain Fresnel zone outward, when the location is close to the Fresnel zone boundary for one subcarrier, we can often exploit the frequency diversity to find another subcarrier showing a well-received signal waveform for the same position (near the middle of the Fresnel zone). For amplitude of activity bigger than wavelength, peaks and valleys will be generated, with the number corresponding to the number of Fresnel zones crossed, when body part crosses the Fresnel zones. The number of Fresnel zones crossed can be measured by counting the peaks and valleys of the received signal using fast Fourier transform.

In the WiDriver, Wi-Fi signal frequency is 2.4 GHz, the wavelength λ is about 12 cm. The driver's displacement range is always bigger than λ, or around λ, so the Fresnel zone model can support that driver's operation on wheel can be detected theoretically.

### 2.4 Challenge

There are two key technical challenges shown in the red block diagram in Fig. 3. The first technical challenge is to locate sensitive CSI segments generated by driver operation for identifying the each action from the CSI time series. CSI provides a detailed knowledge of the wireless link, including the current condition of the channel, attenuation and phase shift experienced by each spatial stream to each receive antenna in each of the OFDM subcarriers. Let $M_T$ denote the number of transmit antennas, $M_R$ denote the number of receive antennas and $S_c$ denote the number of OFDM subcarriers. For each Tx-Rx antenna pair, the driver of COTS NIC device reports CSI values for $S_c$ OFDM subcarriers of the *20/40* MHz WiFi Channel. This leads to $S_c$ matrices $CSI_i$ ($i = 1,\ldots,56$) in Eq. 2. The $M_R \times M_T$ dimensional channel matrix $H_i$ represents the CSI data for the sub-carrier $i$. $H_i$, is a complex value given as Eq. 3. $|Hi|$ and $\angle H_i$ $\psi$ are the amplitude and phase response of subcarrier $i$ respectively. The original CSI data directly from commercial NIC include average signal power RSSI, amplitude and phase variance with time wave in diverse subcarriers and between diverse antenna pairs, *we employed BP algorithm to recognize the sensitive input data in CSI matrix for driver activity recognition. In this paper, amplitude with RSS is most sensitive, and amplitude matrix only is more sensitive than RSS or phase matrix.*

$$CSI = \begin{cases} RSSI : \left[M_R \times M_T \ u\_int8\_t\right] \\ H_i : \left[M_R \times M_T \ complex \ double\right] \end{cases} \quad i \in \left[1, S_c\right] \tag{2}$$

$$H_i = |H_i| \exp\left(j \angle H_i\right) \tag{3}$$

The second technical challenge is to design an effective action recognition algorithm to analyze the current operation action of the driver on time based on sensitive input data. *We introduced DCMA model describing driver action context finite automate to track the driver motion in real time.*

## 3 Sensitive Input Data Analysis

This paper explores the properties of the channel state information (CSI) of Wi-Fi signals acquired from COTS devices, and choose the most cost-effective sensitive data original for recognizing the driver operation maneuver.

Let $X_i$ and $Y_i$ represent the $M_T$ dimensional transmitted signal vector and $M_R$ dimensional received signal vector, respectively, for subcarrier $i$ and let $N_i$ represent an $M_R$ dimensional noise vector. An $M_R \times M_T$ MIMO system at any time instant can be represented in the frequency domain by the following equation.

$$Y_i = H_i X_i + N_i \quad i \in \left[1, S_c\right] \tag{4}$$

Each channel matrix entry in $H_i$ is a complex number, with signed 8-bit resolution each for the real and imaginary parts. It specifies the gain and phase of the signal path between a single transmit–receive antenna pair.

$$H_i = \begin{bmatrix} \left\langle |H|_{1,1}, \angle H_{1,1} \right\rangle & \cdots & \left\langle |H|_{M_T,1}, \angle H_{M_T,1} \right\rangle \\ \vdots & \cdots & \vdots \\ \left\langle |H|_{1,M_R}, \angle H_{s,1} \right\rangle & \cdots & \left\langle |H|_{M_T,M_R}, \angle H_{M_T,M_R} \right\rangle \end{bmatrix}_i \tag{5}$$

Any two communicating Wi-Fi devices estimate this channel matrix $H_i$ for every subcarrier by regularly transmitting a known preamble of OFDM symbols between each other. CSI captures rich wireless channel characteristics such as shadowing fading, distortion, and the multipath effect.

### 3.1 Data from CSI in WiDriver

In our WiDriver, we use two laptop embedded with Atheros AR9580 NIC, and one is configured as router to send packets at regular intervals with $\tau_i$, the other works as receiver to record the CSI uploaded by NIC driver. The duration of each posture is $\tau_p$. The amount of each collection of packets is $N_p$. The working parameters in WiDriver are listed in Table 1. Every $\tau_p/\tau_i$ data packages are put together as one input group.

The received CSIs are big matrices, including multi-dimension information shown in Eq. 2. We can get the RSSI matrices, amplitude matrices and phase matrices in specified subcarriers. CSIs contain information that characterizes the in-car environment they pass through. If a driver make different operation in the car, additional signal paths

**Table 1** Working parameters of WiDriver

| Parameter | Value | Parameter | Value |
|---|---|---|---|
| $M_T$ | 1 | $M_R$ | 3 |
| $S_c$ | 56 | *WiFi band* | 20 MHz |
| $\tau_i$ | 200 μs | $\tau_p$ | 1 s |
| $N_p$ | 300 thousand packets | | |

or path changes are introduced by the scattering of human arms and hands. Then, the received signals also convey information that characterizes the effects of driver's action in the environment. Figure 4 describes the amplitudes of the original CSI waveform of p1and p4 in subcarrier 2 and 18. We can conclude that amplitude matrices from subcarrier 2 is more sensitive than amplitude from subcarrier 18. There are almost no data overlap in Fig. 4a, but the data from subcarrier 18 of different posture have approximate value, and cannot be used to distinguish the p1 and p4 at all.

In WiDriver, Wi-Fi signal affected by driving activities of 5 participants were measured. Each participant in our CSI sampling performs 11 diverse static postures on wheel, and 5 continuous driving operations. There are $Sc \times M_T \times M_R$ CSI stream in a time-series of CSI value. For each posture or action, the WiDriver sampled 120 thousands to 150 thousands CSI stream. There are totally 2 million CSI data matrices, and every data has labeled. Parts of the dataset can be downloaded from [24].

CSI matrices are big, and can be arranged and combined in many kinds of data. So the problem is how to find out the most sensitive data as input of driver action recognition algorithm?

## 3.2 The Method of Selecting Most Sensitive Input

We certificate the sensitive input by leveraging offline BP (back propagation) neural network algorithm. BP neural network is a kind of most widely applied neural network models that consists of input layer, hidden layer and output layer. It can be used to model complex relationship between inputs and outputs or to find patterns in data.

The multi-layer BP network is built in WiDriver, suppose its input node is $I_i(i \in [1,n])$, the node of hidden layer is $H_j(j \in [1,k])$, and the node of output layer is $O_l(l \in [1,m])$. The weight value of network between the input node and node of hidden layer is $w_{ji}$, and the weight value of network between the nodes of hidden layer and output layer is $v_{lj}$. The bias $-\theta$ of each unit is implemented as the weight of an additional edge. When the expected value of the output node is $t_l, f(\cdot)$ is the active function. The computational formula of the model is expressed in Fig. 5

CSI matrix sampled from in WiDriver are multi-dimensional and non-linear [23]. BP is among the nonlinear supervised learning algorithms which can effectively reduce dimensions. We build BP classifier to analyze subset of the entire original CSI set to seek for more efficient combination input. BP is used to train diverse Wi-Fi signal samples and classify the driver posture to see which combination of CSI matrices is most sensitive for recognizing driver activities.

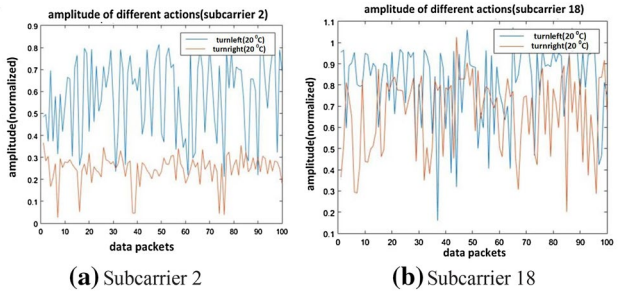


**(a)** Subcarrier 2 **(b)** Subcarrier 18

**Fig. 4** WiDriver schematic **a** CSI waveform in subcarrier 2; **b** CSI waveform in subcarrier 18

**Algorithm.** BP neural network algorithm

1 Forward propagation: output of computer network

1.1 Output of the node of hidden layer

$$H_j = f\left(\sum_i w_{ji} I_i - \theta_j\right) = f(net_j)$$

1.2 Output of the output node

$$O_j = f\left(\sum_j v_{lj} H - \theta_l\right) = f(net_l)$$

1.3 Error of the output node

$$E = \frac{1}{2}\left(\sum_l (t_l - O_l)^2\right) = \frac{1}{2}\left(\sum_l (t_l - f\left(\sum_j v_{lj} f\left(\sum_i w_{ji} I_i - \theta_j\right) - \theta_l\right))^2\right)$$

2 Back propagation: : the gradient descent method is adopted to regulate the weight value of all layers

2.1 Derivation of output node by means of error function

$$\frac{\partial E}{\partial v_{lj}} = \sum_{k=1}^{n} \frac{\partial E}{\partial O_k} \cdot \frac{\partial O_k}{\partial v_{lj}} = \frac{\partial E}{\partial O_l} \cdot \frac{\partial O_l}{\partial v_{lj}}$$

$$\frac{\partial E}{\partial O_l} == \frac{1}{2}\left(\sum_k [-2(t_k - O_k) \cdot \frac{\partial O_k}{\partial O_l}] = -(t_l - O_l)\right)$$

$$\frac{\partial O_l}{\partial v_{lj}} = \frac{\partial O_l}{\partial net_l} \cdot \frac{\partial net_l}{\partial v_{lj}} = f'(net_l) \cdot H_j$$

$$\frac{\partial E}{\partial v_{lj}} = -(t_l - O_l) \cdot f'(net_l) \cdot H_j$$

2.2 Deviation of the node of hidden layer by error function

$$\frac{\partial E}{\partial w_{ji}} = \sum_l \sum_j \frac{\partial E}{\partial O_l} \cdot \frac{\partial O_l}{\partial H_j} \cdot \frac{\partial H_j}{\partial w_{ji}}$$

$$\frac{\partial E}{\partial w_{ji}} = -\sum_l (-(t_l - O_l) \cdot f'(net_l) \cdot v_{lj} \cdot f'(net_j) \cdot I_i$$

3 Modification of weight value: As the modification of weight $\Delta v_{lj}$ and $\Delta w_{ji}$ is in proportion to the error functions and descends along the gradient, the formula showing the modification of weight of hidden layer and output layer. And η represents the learning rate.

3.1 the modification between the input layer and hidden layer

$$\Delta v_{lj} = -\eta \frac{\partial E}{\partial v_{lj}}$$

3.2 the modification between the output layer and hidden layer

$$\Delta w_{ji} = -\eta' \frac{\partial E}{\partial w_{li}}$$

**Fig. 5** BP alogorithm for certificating the most sensitive input from CSI

The investigation of the performance of BP classifier will be applied to consider the effect of the different subset in CSI matrices. The result is detailed in Sect. 5.1.

## 4 Action Recognition Algorithm Based on DCFA

To remind the drivers that dangerous vehicle maneuvers or correct maneuvers following the route, we consider driver 7 continuous actions and 1 default action, defined in Fig. 2. Continuous actions can be described as static posture sequences over a time period. The recognition algorithm of continuous action in our WiDriver consists of the following two key schemes, first is defining action recognition rules, that is the relationship between postures sequence with duration time and different actions. The second is establishment of Driver Context finite automata (DCFA) Model.

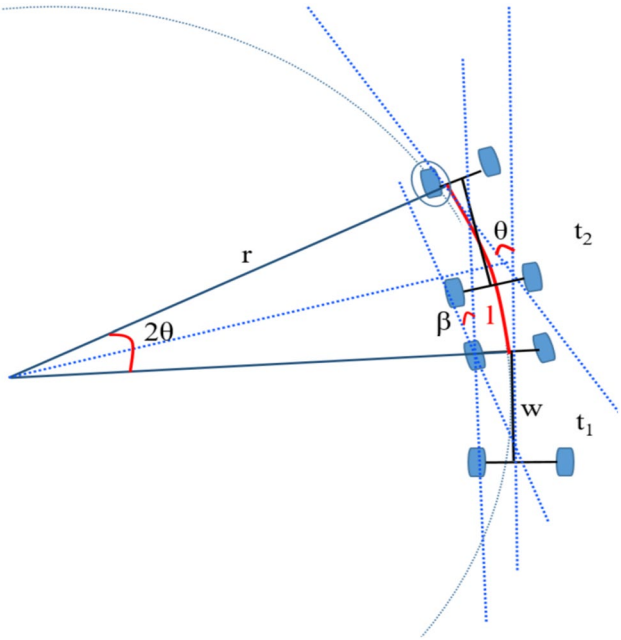


**Fig. 6** Simplified maneuver model for defining the continuous actions

### 4.1 Postures Time Sequence in Diverse Continuous Actions

Design of continuous action classification is based on the analysis of postures sequence and the duration of the postures. The WiDriver leverages the simplified maneuver model shown in Fig. 6 to define the relationship between posture sequences and continuous actions. Figure 6 describes steering angle computation during the wheel maneuver of turning left. At time $t_1$, the driver starts rotating the steering wheel to the left, and at the time $t_2$, The rotation angle of the steering wheel is $\Delta\alpha$; $\beta$ is defined as the deflection angle of the steering wheel of the vehicle; N is the constant ratio of $\Delta\alpha$ to $\beta$, shown in Eq. 6. w is the wheelbase of the vehicle; r is the radius of rotation of the vehicle, and can be deduced from Eq. 7. Assuming that the vehicle is moving at a uniform speed of v, the time of travel is $t = t_2 - t_1$, we can use Eq. 8 to get the distance traveled by the vehicle l, which is the length of the arc. The angle of vehicle deflection from original route is $\theta$, shown in Eq. 9. $\theta$ is the half of the central angle corresponding to l, shown as the red line in Fig. 6.

$$\beta = \frac{\alpha\Delta}{N} \tag{6}$$

$$r = \frac{w}{\sin\beta} \tag{7}$$

$$l = v \times t \tag{8}$$

$$\theta = \frac{l * 180}{\pi * r * 2} \tag{9}$$

The WiDriver defines the relationship between $\theta$ and different actions. When $|\theta| < 20^{o}$, the action is changing the lane; $90° \geq |\theta| \geq 45°$, the action is turning; and when $|\theta| \geq 90°$, the action is making U-turn. The said equations show that $\theta$ is related with $\Delta\alpha$ and t, and $\Delta\alpha$ is related with posture sequence. The WiDriver simplify the action recognition rules using the fixed parameters, including v = 20 km/h, N = 8. So the action classification rules can be described in Table 2.

**Table 2** Postures sequence and duration time of continuous action

| Continuous action | Posture sequence | Duration |
|---|---|---|
| Go straight | <p1…p1> | > 0.25 s |
| Change lane to left | <(p2\|p4\|p6)…(p2\|p4\|p6)> | 1–2.75 s |
| Change lane to right | <(p3\|p5\|p7)…(p3\|p5\|p7)> | 1–2.75 s |
| Turn left | <(p2\|p4\|p6\|p12\|p14)…(p2\|p4\|p6\|p12\|p14)> | > 2.75 s |
| Turn right | <(p3\|p4\|p7\|p13\|p15)…(p3\|p5\|p7\|p13\|p15)> | > 2.75 s |
| U turn | <(p2\|p4\|p6\|p12\|p14)…(p8\|p3\|p5)…(p2\|p4\|p6\|p12\|p14)> | > 2.75 s |
| Phone call | <p10…p10> | > 0.25 s |
| Send message | <p11…p11> | > 0.25 s |

### 4.2 Driver Context Finite Automata (DCFA) Model

Understanding driver's complex operation on steering wheel requires identifying not only each current posture but also capturing the temporal dependencies which benefits when the detection of driver activity fails due to either poor tracking results, occlusion, background clutter, and so on. The transformation relationship between diverse static postures is studied and DCFA model is proposed for optimizing recognition algorithm of continuous actions.

The WiDriver describe the logical transformation relationship as Driver posture shift Context Finite Automata (DCFA) model, according to temporal sequence of postures in some specified continuous maneuver action. The CSI sample interval $\tau_i$ of WiDriver is 200 μs In normal vehicle maneuvers, objectives change postures at least every 1 s, the posture duration time is defined as $\tau_{np} = 1$ s. So there should be causal connections between static postures. For example, after p4 = <turn right-wheel = 20°> , it is possible to transform to p5 = <turn right-wheel = 40°> , or p6 = <turn right-wheel = 60°> , or p1 = <stay-wheel = 0°> , but it is unreasonable to transform to p3 = <turn left-wheel = − 20°> , or p8 = <turning left-wheel: − 270°> .

Figure 7 describes the DCFA model in normal vehicle maneuvers.

1. The posture sets is extended for distinguish different continuous actions. The supplemented postures are p12 = < turning left-wheel: − 120°> , p13 = <turning right-wheel: +120°> , p14 = < turning left-wheel: − 180°> , p15 = <turning right-wheel: +180°>. More posture classes mean longer classification time.
2. The actions are graded into first step class T1, steer left class T2 and steer right class T3. From a1 = go straight, there are first step class actions T1, including steer left, steer right and a6 = phone call, a7 = sending message. After steer left, actions in T2 can be done, driver can do a1 = change lane from right to left, a3 = turn left or a5 = make U turn.
3. Every normal vehicle maneuver is a continuous posture sequence; such as action a6 = calling includes posture P10 = <raise and call-wheel = 0°>. Steer left includes P2 = <turn left-wheel = − 20°> nd P4 = <turn left-wheel = − 40°>. Actions exist different level, posture shift conforms to driver operation context connected with lines shown in Fig. 7.

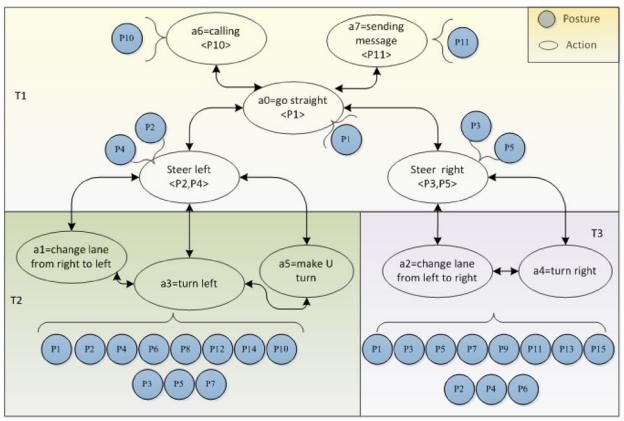


**Fig. 7** DCFA model in normal vehicle maneuvers

### 4.3 Design of Contiuous Action Classifier Based on DCFA

The WiDriver explores the posture sequences and DCFA model to build the Continuous Action Classifier (CAC_DCFA) The algorithm include following steps shown in Fig. 8. After recognizing the current posture, the WiDriver leverages posture shift temporal relationship to decide the driver maneuver actions. DCFA model is introduced to simplify the posture recognition progress.

In order to speed up the algorithm and improve classification accuracy. The WiDriver leverage DCFA model into the step 2 to optimize the scheme. According to DCFA, we can cut down set of posture types from some specified posture. The WiDriver has three posture BP schemes for three level driver postures, so unreasonable states are ruled out. Also, CAC-DCFA can employ the DCFA to double check the posture shift sequence using confirmation window Δt, which is detailed in Fig. 9.

**Algorithm.** Continuous Action Classifier based on Posture Sequence

1 Build BP-based posture classifier after BP offline training algorithm on static posture datasets by two objectives.
2 Detect current posture by leveraging BP-based posture classifier
3 Track and log duration of posture.
4 Analyze the posture sequences and duration to decide the driver maneuver according to table 2.

**Fig. 8** Continuous action classifier algorithm

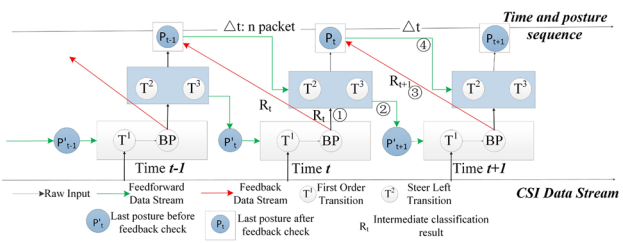


**Fig. 9** Algorithm of CAC-DCFA

**Table 3** Input subset from original CSI

| | Input subset definition |
|---|---|
| $\|H\|$ | $\|H\| = \|H_i\| : \left[M_R \times M_T \ \ complex\ double\right] \quad i \in \left[1, S_c\right]$ |
| $\angle H$ | $\angle H = \left\{\angle H_i : [M_R \times M_T \ \ complex\ double\right\} \quad i \in [1, Sc]$ |
| RSSI | $M_R \times M_T u\_int8\_t$ |
| $M_{all}$ | $M_{all} = \begin{cases} RSSI : \left[M_R \times M_T u\_int8\_t\right] \\ H_i : \left[M_R \times M_T \ \ complex\ \ double\right] \end{cases} \quad i \in [1, Sc]$ |
| $M_{amplitude+RSSI}$ | $M_{amplitude+RSSI} = \begin{cases} RSSI : \left[M_R \times M_T u\_int8\_t\right] \\ \|H_i\| : \left[M_R \times M_T complex\ double\right] \end{cases} \quad i \in [1, Sc]$ |
| $M_{phase+RSSI}$ | $M_{amplitude+RSSI} = \begin{cases} RSSI : \left[M_R \times M_T u\_int8\_t\right] \\ \|H_i\| : \left[M_R \times M_T complex\ double\right] \end{cases} \quad i$ |

At certain time t, the posture classification is proceeded by BP mechanism, including the following three steps:

1. The most sensitive raw CSI data is extracted as the input of the $T^1$ BP classifier, another input is the last posture $P'_t$ given by $T^2$ or $T^3$ BP classifier at time $t-1$. The intermediate posture classification result is outputted by $T^1$ BP classifier to the $T^2$ or $T^3$ BP classifier at time $t-1$ for double check of posture at time $t-1$. The final last posture is recognized as $P_{t-1}$.
2. $T^2$ or $T^3$ BP classifier at time t leverages the $P_{t-1}$ and current CSI data to output current posture $P'_{t+1}$ as one input of the next $T^1$ BP classifier.
3. The result of $T^1$ BP classifier at time $t+1$ will be used to amend posture classification at time t.
4. The final confirmed posture will be input to next $T^2$ or $T^3$ BP classifier at time $t+1$ for next posture detection.

## 5 Experiments and Results

The WiDriver builds offline BP verifier to confirm the most sensitive input, and introduce DCFA model to build continuous action classifier to detect vehicle maneuver. 90% data in CSI datasets were used in training and 10% were used in validation.

### 5.1 Selection of Sensitive Input from Original CSI

Original CSI is a fine-grained time domain RF characteristic set, this paper arrange and combine the subset of CSI as the BP classifier input shown in Table 3. The diverse input makes the classifier to achieve the different recognition accuracy, shown in Fig. 10. Also, the process times of classifier with different input are counted as shown in Fig. 11. Input preparation time means the cost of converting the data structure from CSI tool into the input required by the BP network classifier. Computing time means the time it takes to output data by the BP classifier.

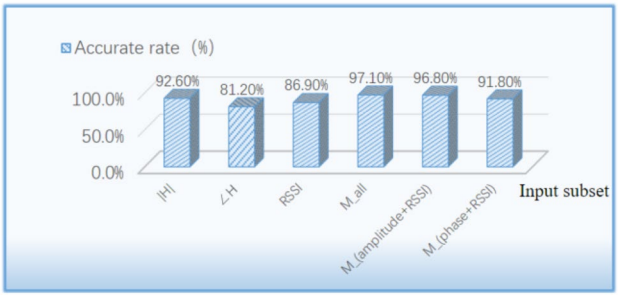


**Fig. 10** BP recognition rate based on different input dataset

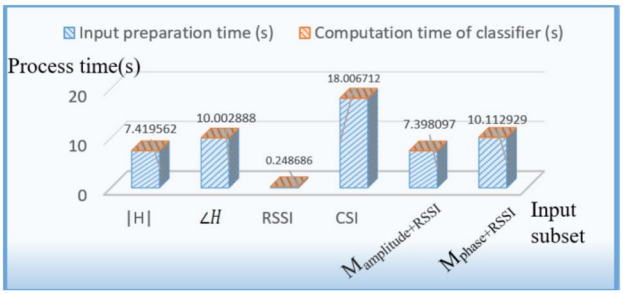


**Fig. 11** BP process time based on different input dataset

According to Figs. 10 and 11, the WiDriver selects the most sensitive and cost-effective input subset data $M_{amplitude+RSSI}$. From Fig. 11, using $M_{all}$ including all dataset of original CSI data as the input of the driver posture classifier get the highest recognition rate 97.1%, also take the longest process time with 18 s shown in Fig. 11. $M_{amplitude+RSSI}$ is second sensitive input data for posture recognition, the accuracy rate is high as 96.8%, and just takes 7.3 s shown in Fig. 11, less than half time of $M_{all}$ as input, so $M_{amplitude+RSSI}$ is the best choice according to sensitivity and cost-effectiveness.

*Conclusion 1* $M_{amplitude+RSSI}$ is more sensitive than *RSSI* only.

From Fig. 10, using the amplitude matrices from original CSI data with RSSI as the input of the driver posture classifier get the high recognition rate 96.8%. Using *RSSI* only just get 86.9% accuracy rate from Fig. 10. $M_{amplitude+RSSI}$ is more sensitive than *RSSI* only. The reason is frequency-selective fading.

CSI amplitude matrix include all detailed subcarrier signal energy. *RSSI* is a measurement average, storing the received energy of combination of all active chain. As shown in Fig. 4, we find that certain channels in 802.11n wireless transmission may be vulnerable to motion of driver arms and hands, but the data variance of channel data in some other channels may be minus. RSSI cannot indicate the biggest change by averaging and reducing the change margin.

802.11n wireless network leverages OFDM system with spacing between sub-carries such that no inter-channel interface occurs for the worst case channel scenario (Low coherence bandwidth). The coherence bandwidth of the channel is smaller than the bandwidth of the signal. Different frequency components of the signal therefore experience uncorrelated fading. frequency-selective fading, As the carrier frequency of a signal is varied, the magnitude of the change in amplitude will vary. The coherence bandwidth measures the separation in frequency after which two signals will experience uncorrelated fading.

*Conclusion 2:* CSI amplitude set is more sensitive than CSI phase set.

From Fig. 10, using the phase matrix as the input of the driver posture classifier get the lowest recognition rate 81.8%. The reason is that the actual measured CSI contains not only the channel information but also the error generated when the signal is received, due to the limitations of the receiver work mode and received signal format. The error makes the phase information of the CSI unusable directly, unless additional hardware and software processing logic is supplemented.

### 5.2 Classification Accuracy of Driver Continuous Action

5 objectives drived in the car on the road for verification of continuous action recognition. As shown in Fig. 12, the WiDriver has a pretty high accuracy rate in the recognition of normal steering maneuvers and other two phone-related actions.

The recognition of CAC_DCFA algorithm get obvious more accurate classification rate. For recognizing lane-changes to the left, the accuracy rate reaches 94%; while for recognizing right turning, the accuracy rate is 95.6%. Figure 13 compares the accuracy of algorithm with and without DCMA model, obviously without DCFA model, algorithm is not high enough, because the actions of phone calling and sending message confuse the judgement of all the actions of

Steering recognition results of CAC_DCFA algorithm

| eering patterns | phone call | send messages | Change left lane | Change right lane | Turn left | Turn right | U-turns |
|---|---|---|---|---|---|---|---|
| phone call | 1.00 | 0 | 0 | 0 | 0 | 0 | 0 |
| send messages | 0 | 0.9 | 0 | 0 | 0.10 | 0 | 0 |
| hange left lane | 0 | 0 | 0.94 | 0 | 0.05 | 0.01 | 0 |
| Change right lane | 0 | 0 | 0.05 | 0.85 | 0.05 | 0.05 | 0 |
| Turn left | 0 | 0 | 0.067 | 0.067 | 0.867 | 0 | 0 |
| Turn right | 0 | 0 | 0 | 0.035 | 0.01 | 0.956 | 0 |
| U-turns | 0 | 0 | 0.05 | 0 | 0.10 | 0.01 | 0.84 |

**Fig. 12** Recognition rate of CAC_DCFA algorithm

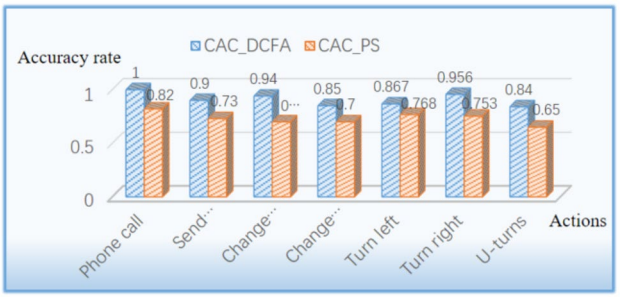


**Fig. 13** Comparation of accuracy rate of algorithm with and without DCFA model

turning the wheel to the left and small range right-turning operation. Also, without the constraint of driving context, the false posture classification rate is some higher, so the action detection accuracy rate based on posture classification is obviously lower.

## 6 Conclusions

This paper proposes WiDriver, a system to employ original CSI variation data to intelligently estimate driving actions with commodity WiFi devices. we define set of the static posture and continuous action in common driver operation on steering wheel. We build BP verifier to analyze the huge original CSI data variance related with the driver action, and find out the combination of CSI amplitude matrix $|H_i|$ and RSSI vector is most sensitive data for recognition of driver common operation maneuver. Classification accuracy of 11 static driver postures based on $|H_i| + RSSI_i$ is found to be around 96.8%. The major contributions of this paper are proposing a DCFA model to show reasonable driver activity shift context. The model is put forward into

back-propagation neural networks algorithm to track sequential motion of driver. Recognition accuracy for classifying continuous operation action is about averagely 90.76%.

The future work may include: extending driver activity related CSI dataset with more candidates for improvement of applicability; enriching driver operation activity set with more actions for improvement of practicality; the implementation and comparison of multiple algorithms for achievement of higher classification rate for all candidate driver activities on time.

**Acknowledgements** This work is supported by National Natural Science Foundation of China (NSFC) Project Nos. 61671056, 61302065, 61304257, 61402033, Beijing Natural Science Foundation Project No. 4152036 and the Fundamental Research Funds for the Central Universities No. FRF-TP-15-026A2.

## References

1. H. Veeraraghavan, S. Atev, N. Bird, et al., Driver activity monitoring through supervised and unsupervised learning. In *Intelligent Transportation Systems, 2005, Proceedings. 2005 IEEE*, 2005, pages 580–585. IEEE
2. Martin S, Ohn-Bar E, Tawari A, et al., Understanding head and hand activities and coordination in naturalistic driving videos. In *Intelligent Vehicles Symposium Proceedings, 2014 IEEE*, pages 884–889, 2014. IEEE
3. C. Braunagel, E. Kasneci, W. Stolzmann, et al., Driver-activity recognition in the context of conditionally autonomous driving. In *Intelligent Transportation Systems (ITSC), 2015 IEEE 18th International Conference on. IEEE*, pages 1652–1657, 2015.
4. S. Park, M. Trivedi Driver activity analysis for intelligent vehicles: issues and development framework. In *Intelligent Vehicles Symposium, 2005. Proceedings. IEEE*, pages 644–649, 2005. IEEE
5. Y. Geng, J. Chen, R. Fu, et al., Enlighten wearable physiological monitoring systems: on-body rf characteristics based human motion classification using a support vector machine, *IEEE Transactions on Mobile Computing*, Vol. 15, No. 3, pp. 656–671, 2016.
6. F. Caba Heilbron, J. Carlos Niebles, and B. Ghanem, Fast temporal activity proposals for efficient detection of human actions in untrimmed videos. In *Proceedings of the IEEE Conference on Computer Vision and Pattern Recognition*, pages 1914–1923, 2016.
7. J. He, Y. Geng, Y. Wan, et al., A cyber physical test-bed for virtualization of RF access environment for body sensor network, *IEEE Sensors Journal*, Vol. 13, No. 10, pp. 3826–3836, 2013.
8. Q. Pu, S. Gupta, S. Gollakota, et al. Whole-home gesture recognition using wireless signals. In *Proceedings of the 19th Annual International Conference on Mobile Computing and Networking*, pages 27–38, 2013. ACM.
9. F. Adib, Z. Kabelac, D. Katabi, and R. C. Miller, 3D tracking via body radio reflections. In *Proceedings of the 11th USENIX Conference on Networked Systems Design and Implementation, Seattle, WA, USA*, 2–4 April 2014; pages 317–329.
10. D. Halperin, W. Hu, A. Sheth, et al., Tool release: gathering 802.11 n traces with channel state information, *ACM SIGCOMM Computer Communication Review*, Vol. 41, No. 1, pp. 53–53, 2011.
11. Y. Xie, Z. Li, and M. Li, Precise power delay profiling with commodity wifi. In *Proceedings of the 21st Annual International Conference on Mobile Computing and Networking*, pages 53–64, 2015. ACM
12. C. Han, K. Wu, Y. Wang, and L. M. Ni, Wifall: Device-free fall detection by wireless networks. In *Proceedings of the IEEE INFOCOM, Toronto, ON, Canada*, 27 April–2 May 2014, pages 271–279.
13. Y. Wang, J. Liu, Y. Chen, M. Gruteser, J. Yang, and H. Liu, E-eyes: Device-free location-oriented activity identification using fine-grained wifi signatures. In *Proceedings of the 20th annual International Conference on Mobile Computing and Networking, Maui, HI, USA*, 7–11 September 2014; pages 617–628, 2014.
14. C. C Li, and S. H. Fang, Device-free human detection using WiFi signals. In *Consumer Electronics, 2016 IEEE 5th Global Conference on*, pages 1–3, 2016. IEEE
15. W. Xi, J. Zhao, X. Y. Li, et al., Electronic frog eye: Counting crowd using wifi. In *Infocom, 2014 proceedings IEEE*, pages 361–369, 2014. ACM.
16. G. Wang, Y. Zou, Z. Zhou, et al., We can hear you with wi-fi!, *IEEE Transactions on Mobile Computing*, Vol. 15, No. 11, pp. 2907–2920, 2016.
17. K. Ali, A. X. Liu, and W. Wang, et al. Keystroke recognition using wifi signals. In *Proceedings of the 21st Annual International Conference on Mobile Computing and Networking*, pages 90–102, 2015. ACM
18. H. Wang, D. Zhang, J. Ma, et al., Human respiration detection with commodity wifi devices: do user location and body orientation matter?. In *Proceedings of the 2016 ACM International Joint Conference on Pervasive and Ubiquitous Computing*, pages 25–36, 2016. ACM
19. X. Liu, J. Cao, S. Tang, et al., Contactless respiration monitoring via off-the-shelf Wifi devices, *IEEE Transactions on Mobile Computing*, Vol. 15, No. 10, pp. 2466–2479, 2016.
20. C. Xu, J. He, X. Zhang, H. Cai, et.al., A Classification capability quantification method for human activity recognition. *In 2017 IEEE Ubiquitous Intelligence and Computing (UIC 2017)*, Aug 4–8, San Francisco, USA, 2017
21. E. Ohn-Bar, S. Martin, and A. Tawari A, Head, eye, and hand patterns for driver activity recognition. In *Pattern Recognition (ICPR), 2014 22nd International Conference on*, pages 660–665, 2014. IEEE.
22. D. Zhang, H. Wang and D. Wu, Toward centimeter-scale human activity sensing with Wi-Fi signals, *Computer*, Vol. 50, No. 1, pp. 48–57, 2017.
23. S. Palipana, P. Agrawal, and D. Pesch D, Channel state information based human presence detection using non-linear techniques. *BuildSys@ SenSystem*, pp. 177–186, 2016.
24. Dataset of the WiDriver. http://pan.baidu.com/s/1geFSmlX.

**Shihong Duan** received the B.E. and Ph.D. degree in pattern recognition and computer science from University of Science and Technology Beijing (USTB), China in 1998 and 2012, respectively. Since July 2013, she has been an associate professor of the School of Computer and Communication Engineering, USTB, where she was an assistant professor from January 1998 to June 2013. From August 2014 to August 2015, she was a visiting scholar in Center for Wireless Information Network Studies, Department of Electrical and Computer Engineering, Worcester

Polytechnic Institute. Her research interests includes wireless wireless channel study, human activity recognition, mobile robotics.

**Tianqing Yu** a junior student of University of Science and Technology Beijing (USTB). His major is Computer Science and Technology. He shows a great interest in posture recognition and pattern identification based on WiFi signals.

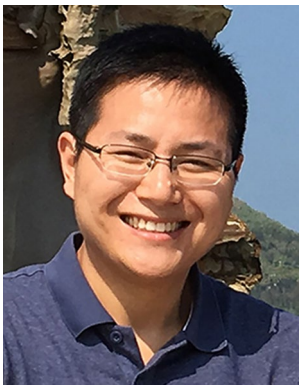

**Jie He (S'11, M'13)** received the B.E. and Ph.D. degree in computer science from University of Science and Technology Beijing (USTB), China in 2005 and 2012, respectively. Since July 2015, he has been an associate professor of the School of Computer and Communication Engineering, USTB, where he was an assistant professor from January 2015 to June 2017 and a postdoctoral researcher from January 2013 to December 2014. From April 2011 to April 2012, he was a visiting Ph.D. student in Center for Wireless Information Network Studies, Department of Electrical and Computer Engineering, Worcester Polytechnic Institute. His research interests includes wireless indoor positioning, human gesture recognition and motion capture.